Superconducting properties of NbTiN thin films deposited by high-temperature chemical vapor deposition

D. Hazra,[1,*] N. Tsavdaris,[2] A. Mukhtarova,[1] M. Jacquemin,[2] F. Blanchet,[1] R. Albert,[1] S. Jebari,[1] A. Grimm,[1] A. Konar,[3]
E. Blanquet,[2] F. Mercier,[2] C. Chapelier,[1] and M. Hofheinz[1]

[1]*Univ. Grenoble Alpes, CEA, INAC, PHELIQS, 38000 Grenoble, France*
[2]*Univ. Grenoble Alpes, CNRS, Grenoble INP, SIMaP, 38000 Grenoble, France*
[3]*GLOBALFOUNDRIES, Bangalore, Karnataka 560045, India*

We report on the superconducting properties of $Nb_{1-x}Ti_xN$ thin films of thickness $\sim$10 nm, with different Ti fraction x in the range $0 \leqslant x \leqslant 0.5$, deposited by high-temperature chemical vapor deposition. In this parameter range, we observe that the superconducting critical temperature (T_c) increases with x. We analyze the possible role played by various parameters—Debye temperature, electron-phonon coupling constant, and Coulomb pseudopotential—in determining the observed variation of T_c with x.

I. INTRODUCTION

Because of its high superconducting critical temperature, high-quality NbTiN has been one of the most preferred materials for many superconducting applications, such as superconducting coating for radio frequency cavities [1–3]. The high superconducting energy gap (Δ) makes NbTiN very suitable for THz applications, such as superconductor-insulator-superconductor mixtures and bolometers [4–7]. NbTiN is also a preferred material for optical single photon detection [8–11] and has been used as high characteristic-impedance microwave resonator [12], thanks to its very high kinetic inductance. Low-loss resonators can be fabricated from NbTiN [13,14]; this in combination with high Δ, T_c, and the upper critical magnetic field B_{c2} make NbTiN a potential alternative to aluminum for circuit quantum electrodynamics in high magnetic fields [12].

The effect of disorder on conventional s-wave superconductivity has been extensively studied in $Nb_{1-x}Ti_xN$ and its parent compounds, NbN and TiN [15–27]. Already vast and rich physics has been unearthed in these systems, including superconductor-insulator transition [15,17], observation of a pseudogap regime above T_c [20,21], disorder-induced phase fluctuation [21], spatially inhomogeneous superconductivity [19,26,27], and enhancement of the pair breaking parameter [23].

Despite numerous applications and fundamental investigations, the following points are clearly missing: (1) a controlled growth technique to deposit high quality thin films, (2) a clear understanding of the variation of superconducting parameters with Ti fraction (x), and (3) a systematic way to control electronic disorder and to study its effect on superconducting properties. Here, we report on the superconducting properties of high-quality $Nb_{1-x}Ti_xN$ films where electronic disorder can be tuned by controlling x. We study the variation of T_c

with x and analyze the role that can be played by Debye temperature, electron-phonon coupling constant, and Coulomb pseudopotential.

Variations of superconducting parameters, especially T_c, with Ti fraction x have been previously reported [28]. The authors observed that T_c remains almost constant up to $x \sim 0.5$ and decreases for higher values. In contrast, Myoren *et al.* [29] observed a monotonic decrease of T_c with x for three of their films with $x = 0, 0.34$, and 0.62, respectively. In both cases, the films constituted three-dimensional systems with thicknesses above 300 nm and were prepared by dc magnetron sputtering. Prior to these experiments, Pressal *et al.* [30] and Yen *et al.* [31] observed that T_c varies nonmonotonically with x; below $x \sim 0.4$, T_c increases with x and decreases above. In either of these cases, no systematic analysis for the observed variation of T_c with Ti fraction was done.

To study the effect of disorder on superconducting properties, the majority of experiments have been focused on series of films with different thicknesses, making it difficult to disentangle bulk disorder from surface scattering contributions. Moreover, to grow $Nb_{1-x}Ti_xN$ thin films, dc magnetron sputtering is the most common technique [12,14,32–36] and the high sputtering rate makes thickness control very challenging below 10 nm. Atomic layer deposition (ALD) has also been explored [37], but in this case the control of both composition and crystalline quality remains difficult.

Here, to overcome these issues, we report on the superconducting properties of five $Nb_{1-x}Ti_xN$ thin films of thickness 10 nm grown by high-temperature chemical vapor deposition (HTCVD). The detailed structural analysis by x-ray diffraction and cross-sectional high-resolution transmission electron microscopy reveal that the deposited films are of very high crystalline quality. Apart from different gas flow rates, chamber conditions are kept identical between depositions. In this way, the only parameter changing from sample to sample is the Ti fraction (x), which we control in the range $0 \leqslant x \leqslant 0.5$ for the present study. Our goal is to explore how x, in this range,
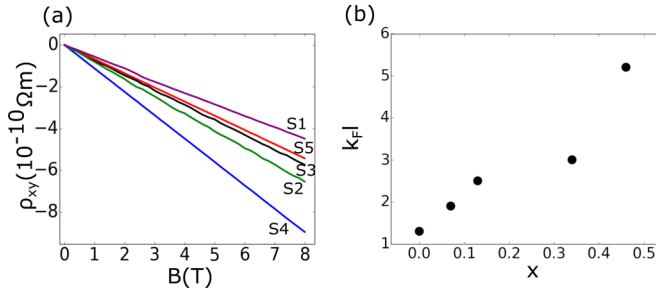
FIG. 1. (a) ρ_{xy} for all five samples at 50 K as a function of magnetic field. (b) The variation of Ioffe-Regel parameter ($k_F\ell$), determined at 50 K, as a function of Ti fraction (x).

FIG. 2. (a) Temperature dependence of ρ_{xx} for all five samples down to the superconducting transition temperature. (b) The variation of T_c as a function of Ti fraction showing a monotonic dependence.

impacts disorder and T_c. Disorder will be estimated with the Ioffe-Regel parameter $k_F\ell$; here, k_F is the Fermi wave vector and ℓ is the mean free path.

II. EXPERIMENTS AND RESULTS

Five Nb$_{1-x}$Ti$_x$N thin films were produced by HTCVD at 1100 °C on Epiready (0001) oriented Al$_2$O$_3$ substrates. Descriptions of the deposition apparatus and thermodynamics calculation have been reported elsewhere [38]. Deposition conditions are the same for each sample except for the ratio of chlorine species NbCl$_x$/TiCl$_x$ in the gas phase. The control of the Nb/Ti ratio in the gas phase allows controlling the titanium concentration in the layer. All the films are $d = 10 \pm 1$ nm thick, as determined from x-ray reflectometry.

The films are purly cubic NbTiN (ICDD: 01-088-2404); no hexagonal phases were detected. Also, no peaks corresponding to pure NbN and TiN are detected, indicating the absence of demixing for all the Ti compositions investigated. The XRD (111)-ω scan rocking curve values, referring to the tilt angle along the 111 direction between grains, are low and between 190 and 350 arcsec with no clear dependence on Ti fraction. Thus, the crystalline quality of NbTiN is not affected by the presence of Ti. However, two NbTiN in-plane variants with an in-plane twist relationship of 60° are detected in all samples. These in-plane variants result from the stacking of material with a cubic structure (NbTiN) on a hexagonal substrate [surface of (0001) Al$_2$O$_3$]. We found that the domains with a single variant were distributed randomly and have a lateral size of the order of 150 nm [38,39].

Electrical transport measurements were performed in a Quantum Design physical property measurement system down to 2.5 K and up to magnetic field (B) 8 T. The free electron parameters of our samples were determined from the
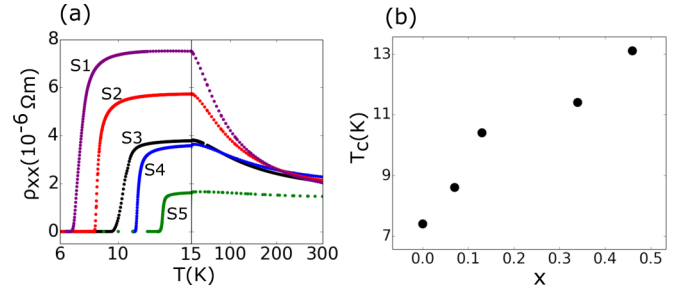
combination of longitudinal and Hall resistivity measurements at 50 K; lower temperatures are avoided in order not to be influenced by superconducting fluctuation related effects [40–42]. Figure 1(a) shows the variation of Hall resistivity (ρ_{xy}) for all five samples as a function of magnetic field. For all five samples, ρ_{xy} varies linearly with magnetic field. The free electron density (n) is determined from the slope of the $\rho_{xy}(B)$ curve, i.e., from the Hall coefficient $R_H = 1/ne$, where e is the charge of the electron. Knowing n, k_F and v_F (the Fermi velocity) are determined from $k_F = (3\pi^2 n)^{1/3}$ and $v_F = \hbar k_F/m$, where m is the mass of the electron. The elastic scattering time (τ) is estimated from Drude's formula: $\rho_{xx} = m/ne^2\tau$; here $\rho_{xx} = dR_S$ is the longitudinal resistivity at 50 K. The other important free electron parameters, like ℓ, diffusion constant (D), and density of states at the Fermi level (N_V) are determined from $\ell = v_F\tau$, $D = v_F\ell/3$, and $N_V = mk_F/\hbar^2\pi^2$. $k_F\ell$ then takes the form $k_F\ell = \frac{h}{e^2}\rho_{xx}^{-1}(\frac{9}{8}\pi e R_H)^{1/3}$. We note that $k_F\ell$ depends only on experimentally measured quantities R_H and ρ_{xx}, not on the effective electron mass m. The important free electron parameters are summarized for each sample in Table I. In Fig. 1(b), we plot $k_F\ell$ as a function of x, showing that $k_F\ell$ increases monotonically with x. Thus, the disorder can be tuned systematically by controlling Ti fraction, making these films ideal candidates to study the effect of atomic level disorder on superconducting properties.

In Fig. 2(a), we plot the temperature dependence of ρ_{xx} at zero magnetic field. Upon cooling down from room temperature, ρ_{xx} increases and reaches a maximum at some intermediate temperature T_{max}. Below T_{max}, ρ_{xx} starts to decrease with decreasing temperature due to the onset of superconductivity. The left panel of Fig. 2(a) shows a magnified version near the superconducting transition. Clearly, T_c is systematically increasing with Ti fraction from sample S1 ($x = 0$) to S5

TABLE I. An overview of some of the important parameters of our Nb$_{1-x}$Ti$_x$N thin films. The free electron parameters are determined at 50 K. The directly measured parameters and those extracted from the free electron theory are separated by the vertical line.

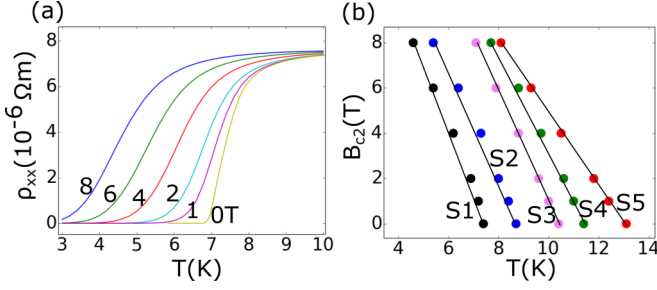| Sample	a (Å)	x	RRR	T_c (K)	R_H (10^{-11} $\frac{m^3}{C}$)	R_S (50 K) (Ω)	$\|\frac{dB_{c2}}{dT}\|_{T=T_c}$ ($\frac{T}{K}$)	n ($\frac{10^{28}}{m^3}$)	τ (10^{-17} s)	ℓ (Å)	$k_F\ell$	D ($\frac{10^{-5} m^2}{s}$)	N_V ($\frac{10^{47} states}{m^3 J}$)	$\xi(0)$ (nm)
S1	4.340	0.00	0.27	7.4	5.6	607	3.23	11.1	5.2	0.9	1.3	5.1	1.24	6.1
S2	4.339	0.07	0.37	8.6	8.4	502	2.60	7.4	9.6	1.4	1.9	7.1	1.10	5.8
S3	4.336	0.14	0.55	10.4	7.9	362	2.41	7.8	12.5	1.9	2.5	9.7	1.10	5.5
S4	4.312	0.34	0.63	11.4	13.8	349	2.30	4.5	22.4	2.8	3.1	12.0	0.92	5.3
S5	4.303	0.46	0.88	13.1	6.8	167	1.60	9.2	23.0	3.7	5.2	19.8	1.17	5.8

FIG. 3. (a) Temperature dependence of ρ_{xx} for S1 at different magnetic fields as indicated in the figure. (b) The variation of B_{c2} as a function of temperature for all five samples. The solid lines are straight-line fits.

FIG. 4. (a) ρ_{xy} for all five samples at 300 K as a function of magnetic field. (b) The variation of the Ioffe-Regel parameter ($k_F\ell$), determined at 300 K, as a function of Ti fraction (x).

($x = 0.5$). This is shown in Fig. 2(b), where T_c is plotted as a function of x. T_c is defined at the temperature where ρ_{xx} is half of normal resistivity defined by ρ_{xx} measured at 15 K. In Table I, we summarize T_c of our samples.

Next, we report the zero temperature Ginzburg-Landau coherence length [$\xi(0)$], which is estimated from the formula $\xi(0) = \sqrt{\Phi_0/2\pi\, T_c |\frac{dB_{c2}}{dT}|_{T=T_c}}$ [43]. For that, magnetoresistance data is collected for all the samples up to a magnetic field of 8 T. In Fig. 3(a), we show the magnetoresistance data for S1, where temperature variation of ρ_{xx} is recorded at five different fields. $B_{c2}(T)$ is determined as the point where ρ_{xx} is half of the normal resistivity. In Fig. 3(b), we plot B_{c2} as a function of temperature. The solid lines are straight-line fits. The slopes and the $\xi(0)$ are listed in Table I.

III. ANALYSIS AND DISCUSSION

We will first focus on Fig. 1(b) which indicates that the disorder of our system decreases, i.e., $k_F\ell$ increases, with x. We note that n and hence k_F decreases with x, except for a sudden anomalous increase for S5. This tells us that the increase of $k_F\ell$ with x is dominated by the increase of ℓ that completely overwhelms the effect of n. This observation is clearly in contradiction with the expected behavior, as it is quite natural that with increasing random doping the disorder scattering should increase, that in turn should reduce ℓ. One possible reason behind this unexpected behavior is that our NbN film, (i.e., S1) contains Nb vacancies and the density of vacancies decreases with increasing Ti concentration. This also appears to be true as we note that S1 ($x = 0$) has a much lower T_c compared to epitaxial NbN films reported in the literature [22,27] with thicknesses 10 nm or less. Here, we would also like to point out that in our structural analysis [38] we observed that surface morphology improves with increasing Ti fraction. This might also facilitate reducing scattering with increasing x. However, a final conclusion on this question requires a detailed compositional analysis, which is beyond the scope of the present work.

Now, we turn our attention to T_c. The T_c of a strongly coupled superconductor like NbTiN is governed by McMillan's equation [44],

$$T_c = \frac{\Theta_D}{1.14}\exp\left(-\frac{1.04(1+\lambda)}{\lambda - \mu^*(1+0.62\lambda)}\right). \qquad (1)$$
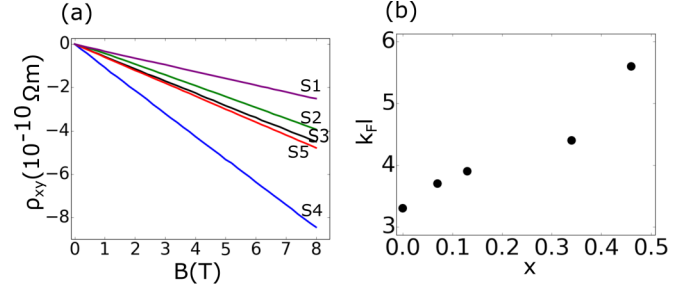
Here, Θ_D is the Debye temperature, λ is the effective electron-phonon coupling constant, and μ^* is the Coulomb pseudopotential representing electronic Coulomb repulsion. λ is given by $\lambda = N_V U$, where U is the attractive potential. Θ_D and U depend on the phonon structure and hence lattice parameter (a) and mass of the unit cell (M_u). μ^*, on the other hand, depends on disorder: with increasing disorder, μ^* increases [45]. Our five samples have different a, M_u, N_V, and $k_F\ell$. In other words, Θ_D, λ, and μ^* are different for all five samples. Thus, it is difficult to analyze the variation of T_c as a function of any single variable Θ_D, λ, or μ^*. In the following, we therefore discuss the possible role that can be played by each parameter.

Let us first focus on Θ_D that, for a monatomic crystal, is given by

$$\Theta_D = \frac{h}{k_B}\left(\frac{3D_a}{4\pi}\right)^{1/3}\left(\frac{Y}{\rho}\right)^{1/2}. \qquad (2)$$

Here, D_a is atomic density, Y is Young's modulus, and ρ is the mass density. Since the difference in lattice parameter from sample to sample is small in our case, D_a does not vary significantly. However, since Nb and Ti have very different atomic masses, 92.9 and 47.9 in atomic units, respectively, ρ would decrease with x. Similarly, Y also depends on x [46]. Thus, it is expected that Θ_D varies with x. In fact, it was observed that Θ_D increases linearly with x, for the entire range of x, with $\Theta_D(x=0) = 634$ K and $\Theta_D(x=1) = 924$ K (see Ref. [46] and references therein); accordingly, the variation of Θ_D is about 20% in our studied range, $0 \leqslant x \leqslant 0.5$.

From the above discussion, we see that although Θ_D varies quite significantly, it is not sufficient to explain alone the observed increase of T_c with x. Since Θ_D represents the characteristic phonon frequency and moreover it is expected that the disorder scattering will smooth finer structures in the phonon spectrum, U and hence λ will also vary from sample to sample. Moreover, unlike Θ_D, λ appears in the exponent in McMillan's equation. Thus, a small change in λ can drastically change T_c.

Finally, we comment on the possible role of μ^* for the observed variation of T_c with x. It is well known that with increasing disorder scattering, Coulomb interaction increases [45]. Since with increasing x, ℓ is increasing for our samples, it is likely that μ^* will decrease with x. Like λ, μ^* also appears in the exponent of McMillan's equation. Thus, μ^* can also play a significant role in determining the variation of T_c with x.

TABLE II. Free electron parameters as determined at 300 K. The directly measured parameters and those extracted from the free electron theory are separated by the vertical line.

Samples	x	R_H $(10^{-11} \frac{\text{m}^3}{\text{C}})$	R_S (300 K) (Ω)	n $(\frac{10^{28}}{\text{m}^3})$	τ (10^{-17} s)	ℓ (Å)	$k_F \ell$	D $(\frac{10^{-5} \text{ m}^2}{\text{s}})$	N_V $(\frac{10^{47} \text{ states}}{\text{m}^3\text{J}})$
S1	0.00	5.6	203	19.8	8.7	1.8	3.3	12.6	1.5
S2	0.07	8.4	212	12.5	13.26	2.4	3.7	714.0	1.3
S3	0.14	7.9	208	11.1	15.3	2.6	3.9	14.9	1.2
S4	0.34	13.8	227	5.9	26.3	3.6	4.4	16.9	1.0
S5	0.46	6.8	146	10.4	23.3	3.9	5.6	21.7	1.12

IV. SUMMARY AND CONCLUSION

In summary, we have studied the superconducting properties of $\text{Nb}_{1-x}\text{Ti}_x\text{N}$ thin films of thickness $\sim$10 nm, with different x in the range $0 \leqslant x \leqslant 0.5$, deposited by high-temperature chemical vapor deposition. In this parameter range, we observe that both $k_F\ell$ and T_c increase with x, suggesting reduced disorder as the source of increasing T_c. However, analysis of the role that can be played by Θ_D, λ, and μ^* in McMillan's framework shows that further investigations are required to uniquely determine the origin of the observed behavior.

APPENDIX

In the main text, we have reported free electron parameters at 50 K where electron-phonon interaction is weaker than at room temperature but electron-electron interaction can be significant [47]. Here, we report free electron parameters determined at 300 K, where electron-electron interaction is weaker than at 50 K [47]. Figure 4(a) shows the variation of ρ_{xy} for all five samples as a function of magnetic field measured at 300 K. The corresponding free electron parameters are summarized for each sample in Table II. In Fig. 4(b), we plot $k_F\ell$ as a function of x, showing that $k_F\ell$ increases monotonically with x as in Fig. 1(b), although the increase is weaker.

[1] C. Benvenuti, P. Chiggiato, L. Parrini, and R. Russo, Nucl. Instrum. Methods Phys. Res., Sect. B **124**, 106 (1997).

[2] P. Fabbricatore, G. Gemme, R. Musenich, R. Parodi, M. Viviani, B. Zhang, and V. Buscaglia, IEEE Trans. Appl. Supercond. **3**, 1761 (1993).

[3] P. Bosland, S. Cantacuzene, J. Gobin, M. Juillard, and J. Martignac, in *Proceedings of the 6th Workshop on RF Superconductivity* (CEBAF, Newport News, Virginia,1993), p. 1028.

[4] J. W. Kooi, J. A. Stern, G. Chattopadhyay, H. G. LeDuc, B. Bumble, and J. Zmuidzinas, Int. J. Infrared Millimeter Waves **19**, 373 (1998).

[5] B. Bumble, H. LeDuc, J. Stern, and K. Megerian, IEEE Trans. Appl. Supercond. **11**, 76 (2001).

[6] B. Jackson, A. Baryshev, G. De Lange, J.-R. Gao, S. Shitov, N. Iosad, and T. Klapwijk, Appl. Phys. Lett. **79**, 436 (2001).

[7] L. Jiang, S. Shiba, T. Shiino, K. Shimbo, N. Sakai, T. Yamakura, Y. Irimajiri, P. Ananthasubramanian, H. Maezawa, and S. Yamamoto, Supercond. Sci. Technol. **23**, 045025 (2010).

[8] S. Miki, T. Yamashita, H. Terai, and Z. Wang, Opt. Express **21**, 10208 (2013).

[9] C. Schuck, W. H. Pernice, and H. X. Tang, Sci. Rep. **3**, 1893 (2013).

[10] M. G. Tanner, C. Natarajan, V. Pottapenjara, J. O'Connor, R. Warburton, R. Hadfield, B. Baek, S. Nam, S. Dorenbos, E. B. Ureña *et al.*, Appl. Phys. Lett. **96**, 221109 (2010).

[11] S. Dorenbos, E. Reiger, U. Perinetti, V. Zwiller, T. Zijlstra, and T. Klapwijk, Appl. Phys. Lett. **93**, 131101 (2008).

[12] N. Samkharadze, A. Bruno, P. Scarlino, G. Zheng, D. P. DiVincenzo, L. DiCarlo, and L. M. K. Vandersypen, Phys. Rev. Appl. **5**, 044004 (2016).

[13] R. Barends, N. Vercruyssen, A. Endo, P. De Visser, T. Zijlstra, T. Klapwijk, P. Diener, S. Yates, and J. Baselmans, Appl. Phys. Lett. **97**, 023508 (2010).

[14] R. Barends, H. Hortensius, T. Zijlstra, J. J. Baselmans, S. Yates, J. Gao, and T. M. Klapwijk, IEEE Trans. Appl. Supercond. **19**, 936 (2009).

[15] A. Goldman and N. Markovic, Phys. Today **51**(11), 39 (1998).

[16] R. Crane, N. P. Armitage, A. Johansson, G. Sambandamurthy, D. Shahar, and G. Grüner, Phys. Rev. B **75**, 184530 (2007).

[17] T. I. Baturina, A. Y. Mironov, V. M. Vinokur, M. R. Baklanov, and C. Strunk, Phys. Rev. Lett. **99**, 257003 (2007).

[18] T. I. Baturina, C. Strunk, M. R. Baklanov, and A. Satta, Phys. Rev. Lett. **98**, 127003 (2007).

[19] B. Sacépé, C. Chapelier, T. I. Baturina, V. M. Vinokur, M. R. Baklanov, and M. Sanquer, Phys. Rev. Lett. **101**, 157006 (2008).

[20] B. Sacépé, C. Chapelier, T. I. Baturina, V. M. Vinokur, M. R. Baklanov, and M. Sanquer, Nat. Commun. **1**, 140 (2010).

[21] M. Mondal, A. Kamlapure, M. Chand, G. Saraswat, S. Kumar, J. Jesudasan, L. Benfatto, V. Tripathi, and P. Raychaudhuri, Phys. Rev. Lett. **106**, 047001 (2011).

[22] M. Mondal, S. Kumar, M. Chand, A. Kamlapure, G. Saraswat, G. Seibold, L. Benfatto, and P. Raychaudhuri, Phys. Rev. Lett. **107**, 217003 (2011).

[23] E. F. C. Driessen, P. C. J. J. Coumou, R. R. Tromp, P. J. de Visser, and T. M. Klapwijk, Phys. Rev. Lett. **109**, 107003 (2012).

[24] P. C. J. J. Coumou, E. F. C. Driessen, J. Bueno, C. Chapelier, and T. M. Klapwijk, Phys. Rev. B **88**, 180505 (2013).

[25] M. Mondal, A. Kamlapure, S. C. Ganguli, J. Jesudasan, V. Bagwe, L. Benfatto, and P. Raychaudhuri, Sci. Rep. **3**, 1357 (2013).

[26] A. Kamlapure, T. Das, S. C. Ganguli, J. B. Parmar, S. Bhattacharyya, and P. Raychaudhuri, Sci. Rep. **3**, 2979 (2013).

[27] Y. Noat, V. Cherkez, C. Brun, T. Cren, C. Carbillet, F. Debontridder, K. Ilin, M. Siegel, A. Semenov, H.-W. Hübers *et al.*, Phys. Rev. B **88**, 014503 (2013).

[28] R. Di Leo, A. Nigro, G. Nobile, and R. Vaglio, J. Low Temp. Phys. **78**, 41 (1990).

[29] H. Myoren, T. Shimizu, T. Iizuka, and S. Takada, IEEE Trans. Appl. Supercond. **11**, 3828 (2001).

[30] N. Pessall, R. Gold, and H. Johansen, J. Phys. Chem. Solids **29**, 19 (1968).

[31] C. Yen, L. Toth, Y. Shy, D. Anderson, and L. Rosner, J. Appl. Phys. **38**, 2268 (1967).

[32] H. Bell, Y. Shy, D. Anderson, and L. Toth, J. Appl. Phys. **39**, 2797 (1968).

[33] R. Barends, H. Hortensius, T. Zijlstra, J. Baselmans, S. Yates, J. Gao, and T. Klapwijk, Appl. Phys. Lett. **92**, 223502 (2008).

[34] K. Makise, H. Terai, M. Takeda, Y. Uzawa, and Z. Wang, IEEE Trans. Appl. Supercond. **21**, 139 (2011).

[35] T. Hong, K. Choi, K. Ik Sim, T. Ha, B. Cheol Park, H. Yamamori, and J. Hoon Kim, J. Appl. Phys. **114**, 243905 (2013).

[36] A. Karimi, D. La Grange, N. Goebbels, and A. Santana, Thin Solid Films **607**, 14 (2016).

[37] J. A. Klug, N. G. Becker, N. R. Groll, C. Cao, M. S. Weimer, M. J. Pellin, J. F. Zasadzinski, and T. Proslier, Appl. Phys. Lett. **103**, 211602 (2013).

[38] N. Tsavdaris, D. Harza, S. Coindeau, G. Renou, F. Robaut, E. Sarigiannidou, M. Jacquemin, R. Reboud, M. Hofheinz, E. Blanquet *et al.*, Chem. Mater. **29**, 5824 (2017).

[39] F. Mercier, S. Coindeau, S. Lay, A. Crisci, M. Benz, T. Encinas, R. Boichot, A. Mantoux, C. Jimenez, F. Weiss *et al.*, Surf. Coat. Technol. **260**, 126 (2014).

[40] K. S. Tikhonov, G. Schwiete, and A. M. Finkel'stein, Phys. Rev. B **85**, 174527 (2012).

[41] N. P. Breznay, K. Michaeli, K. S. Tikhonov, A. M. Finkelstein, M. Tendulkar, and A. Kapitulnik, Phys. Rev. B **86**, 014514 (2012).

[42] D. Destraz, K. Ilin, M. Siegel, A. Schilling, and J. Chang, Phys. Rev. B **95**, 224501 (2017).

[43] M. Tinkham, *Introduction to Superconductivity* (Dover, Mineola, NY, 1996).

[44] W. L. McMillan, Phys. Rev. **167**, 331 (1968).

[45] P. W. Anderson, K. A. Muttalib, and T. V. Ramakrishnan, Phys. Rev. B **28**, 117 (1983).

[46] M. Arockiasamy, M. Sundareswari, and M. Rajagopalan, Indian J. Phys. **90**, 149 (2016).

[47] M. Chand, A. Mishra, Y. Xiong, A. Kamlapure, S. Chockalingam, J. Jesudasan, V. Bagwe, M. Mondal, P. Adams, V. Tripathi *et al.*, Phys. Rev. B **80**, 134514 (2009).